HHS Public Access

Author manuscript

Am J Med Genet A. Author manuscript; available in PMC 2016 April 13.

Published in final edited form as:

Am J Med Genet A. 2015 September ; 167A(9): 2085–2097. doi:10.1002/ajmg.a.37128.

An Attenuated Phenotype of Costello Syndrome in Three Unrelated Individuals with a *HRAS* c.179G>A (p.Gly60Asp) Correlates with Uncommon Functional Consequences

Karen W. Gripp[1,*], **Katia Sol-Church**[2], **Patroula Smpokou**[3], **Gail E. Graham**[4], **David A. Stevenson**[5], **Heather Hanson**[6], **David H. Viskochil**[6], **Laura C. Baker**[1], **Bridget Russo**[2], **Nick Gardner**[2], **Deborah L. Stabley**[2], **Verena Kolbe**[7], and **Georg Rosenberger**[7]

[1]Division of Medical Genetics, A. I. duPont Hospital for Children, Wilmington, Delaware, USA

[2]Center for Applied Clinical Genomics, A. I. duPont Hospital for Children, Wilmington, Delaware, USA

[3]Division of Genetics & Metabolism, Children's National Health System, Washington, District of Columbia, USA

[4]Department of Genetics, Children's Hospital of Eastern Ontario, Ottawa, Ontario, Canada

[5]Stanford University, Division of Medical Genetics, Stanford, CA, USA

[6]Department of Pediatrics, Division of Medical Genetics, University of Utah, Salt Lake City, Utah, USA

[7]Institute of Human Genetics, University Medical Center Hamburg-Eppendorf, Hamburg, Germany

Abstract

Heterozygous germline mutations in the proto-oncogene *HRAS* cause Costello syndrome (CS), an intellectual disability condition with severe failure-to-thrive, cardiac abnormalities, predisposition to tumors and neurologic abnormalities. More than 80% of patients share the *HRAS* mutation c. 34G>A (p.Gly12Ser) associated with the typical, relatively homogeneous phenotype. Rarer mutations occurred in individuals with an attenuated phenotype and less characteristic facial features. Most pathogenic HRAS alterations affect hydrolytic HRAS activity resulting in constitutive activation. 'Gain-of-function' and 'hyperactivation' concerning downstream pathways are widely used to explain the molecular basis and dysregulation of the RAS-MAPK pathway. This is the biologic mechanism shared amongst rasopathies. Panel testing for rasopathies identified a novel *HRAS* mutation (c.179G>A; p.Gly60Asp) in three individuals with an attenuated CS phenotype. De novo paternal origin was documented in two, transmission from a heterozygous mother occurred in the third. Individuals showed subtle facial features; curly hair and relative macrocephaly were seen in three; atrial tachycardia and learning differences in two, and pulmonic valve dysplasia and mildly thickened left ventricle in one. None had severe failure-to-thrive,

[*]Correspondence to: Karen W. Gripp, Division of Medical Genetics, A. I. duPont Hospital for Children, Wilmington, DE 19899, Phone: 302 651 5916, Fax: 302 651 5033, kgripp@nemours.org.

intellectual disability or cancer. Functional studies revealed strongly increased HRAS^{Gly60Asp} binding to RAF1, but not to other signaling effectors. Hyperactivation of the MAPK downstream signaling pathways was absent. Our results and literature data indicate dominant negative consequences of HRAS glycine 60 substitutions on RAS-dependent signaling. We conclude that hyperactivation of RAS downstream signaling does not entirely explain the molecular basis of CS and support the new idea of disrupted HRAS reactivity as a critical molecular dysfunction.

Keywords

Costello syndrome; rasopathy; RAS-pathway disorder; HRAS p.Gly60Asp; Noonan syndrome; *HRAS* germline mutation

INTRODUCTION

Costello syndrome (CS) belongs to the rasopathies, a group of disorders resulting from dysregulation of RAS-depending signaling pathways. Owing to this shared biologic mechanism, there is significant overlap in the phenotype of different rasopathies. This overlap of clinical features can make the clinical differential diagnosis challenging, and molecular confirmation of a clinical diagnosis is often necessary. Costello syndrome is caused by heterozygous germline mutations in the proto-oncogene *HRAS* [Aoki et al., 2005]. It typically encompasses severe failure-to-thrive, cardiac abnormalities including tachyarrhythmia and hypertrophic cardiomyopathy, a predisposition to papillomata and malignant tumors, and neurologic abnormalities including Chiari 1 malformation and tethered cord, nystagmus, hypotonia and intellectual disability [Gripp and Lin, 2006; Gripp and Lin, 2012]. Most patients have an *HRAS* mutation affecting the glycine residue in position 12 [Gripp et al., 2006; Kerr et al., 2006], and the glycine in position 13 is the second most commonly altered amino acid [Gripp et al., 2011a]. Specific amino acid substitutions, particularly those associated with a high transforming activity, may result in an early lethal phenotype [Lo et al., 2008]. In contrast, rarer *HRAS* mutations are associated with an attenuated phenotype as reported for p.Thr58 and p.Ala146 [Zampino et al., 2007; Gripp et al., 2008; Gripp et al., 2012a], or a slightly variant phenotype with p.Glu37dup [Gremer et al., 2010a].

HRAS serves as signal transducer by alternating between an active guanosine triphosphate (GTP)-bound and inactive guanosine diphosphate (GDP)-bound state. The kinetics of GDP dissociation and GTP hydrolysis are modulated by two classes of proteins: Guanine nucleotide exchange factors (GEFs) activate HRAS by mediating the exchange of GDP for GTP, whereas GTPase-activating proteins (GAPs) stimulate the low intrinsic GTPase activity, thereby negatively controlling RAS function [Guo et al., 2005; Scheffzek and Ahmadian, 2005]. In the active state, HRAS binds to a number of effector proteins, such as serine/threonine RAF kinases, the catalytic subunits of phosphoinositide 3-kinase (PI3K), phospholipase C1 (PLCE1) and RAL guanine nucleotide dissociation stimulator (RALGDS) [Karnoub and Weinberg, 2008]. As a result, signal flow via these HRAS target proteins is increased. The functional consequences of mutations of HRAS amino acid 12 were extensively studied due to their prominent role in oncogenic transformation. Such alterations

affect intrinsic and GAP-stimulated hydrolytic HRAS activity and thus maintain its active form decoupled from incoming signals [Fasano et al., 1984; Gideon et al., 1992; Scheffzek et al., 1997; Seeburg et al., 1984]. Therefore, 'gain-of-function' and 'hyperactivation' concerning HRAS downstream signaling pathways are widely used to explain the molecular basis of Costello syndrome. However, the RAS-dependent signaling pathway's intricate regulation defies a simple one dimensional characterization of up and down regulation, as exemplified by the complex effects caused by KRAS sequence changes [Gremer et al., 2010b]. In line with this, functional characterization of rarer HRAS germline mutations revealed additional molecular consequences, including altered GDP/GTP nucleotide affinities (p.Lys117Arg) [Denayer et al., 2008] and inefficient effector binding (p.Glu37dup) [Gremer et al., 2010a]. Notably, a novel pathomechanistic basis of Costello syndrome and related disorders has been added recently: the CS-associated duplication p.Glu63_Asp69dup impairs HRAS reaction to stimuli, resulting in reduced or disrupted transduction of incoming signals to downstream effectors [Lorenz et al., 2013]. By characterizing the novel HRAS p.Gly60Asp mutation, here we provide further evidence that hyperactivation of RAS downstream signaling does not entirely explain the pathomechanistic basis of Costello syndrome. Our data support the new idea of disrupted HRAS reactivity as a phenocritical dysfunction associated with rasopathies.

MATERIAL AND METHODS

CLINICAL REPORTS

Individuals and families were identified through physician referral for Individual 1, through referral from the testing laboratory (GeneDx) for Individual 2, and through physician referral for Individuals 3 and 4 (Family 3). Informed consent was obtained based on protocols approved by the institutional review boards (IRB) at the University of Utah and Nemours. Results were compared to data from a cohort of *HRAS* mutation positive patients enrolled in an ongoing IRB approved study of Costello syndrome at Nemours.

Genomic DNA was extracted from buccal cells from individuals and their respective parents, using Pure Gene DNA Isolation Kit (Gentra Systems, Minneapolis, MN; www.gentra.com). Biologic relationships were confirmed as previously reported [Sol-Church et al., 2006] using microsatellite markers. Sequencing of *HRAS* exons 2, 3, 4 and 5 was performed using primers previously described in Sol-Church et al. [2009]. The families were genotyped around the mutation site in order to identify polymorphic markers to determine the parental origin of the germline mutation. A complete description of the polymorphic markers found in this region is published elsewhere [Sol-Church et al., 2006].

Individual 1 (CS#429)—This female was the first child born to her 41-year old mother and 41-year-old father. Her mother was 157.5 cm and her father was 175.3 cm tall. Both parents were of European ancestry and not consanguineous. She was born at 34-weeks-gestation by cesarian for maternal hypertension and HELLP syndrome. Her birth weight was 1.8 kg (25th centile for gestational age), length 40 cm (3rd centile) and OFC 32.5 cm (75th centile). Apgar scores were 3 at 1 minute and 8 at 5 minutes. She required one dose of surfactant for respiratory distress and was ventilated for 3 days. Hypoglycemia responded to

treatment. Supraventricular tachycardia (SVT) converted to normal sinus rhythm during an eye examination. At age 4 weeks SVT recurred and Holter monitoring showed runs of SVT up to 257 beats/minute with a maximum length of about 900 beats. Propranolol was used to treat the SVT, but bradycardia resulted in a change to digoxin. Echocardiography had normal results. A nasogastric feeding tube was used briefly. Gastroesophageal reflux (GER) was confirmed on imaging studies and treated with medication. She was discharged from the hospital at age 56 days.

Her early motor development was reportedly normal. She required speech therapy from age 2 to 3 years for language delay. Her fine motor skills were good and no formal developmental or cognitive testing was performed. She attended school without accommodations and her performance was age appropriate.

Nystagmus led to a brain MRI performed at age 13 years which showed 2–3 mm cerebellar tonsillar ectopia with “peg-like appearance” and “mild crowding of the structures in the foramen magnum” (Supplemental Fig. 1).

An EKG performed at age 14 years showed normal sinus rhythm. A repeat echocardiogram showed a structurally normal heart with mild encroachment from a pectus excavatum. Menarche had not occurred prior to age 15.5 years, and delayed puberty resulted in an endocrinology evaluation. Low bone mineral density was noted on dual energy x-ray absorptiometry (DEXA) scan and was treated with supplemental vitamin D.

At age 15 3/12 years her height was 149.8 cm (3rd centile), weight 38.4 kg (3rd–5th centile), and OFC 55.5 cm (75–90th centile). She had thick curly hair. Her facial features included apparent hypertelorism and mild bilateral ptosis, posteriorly angulated ears and prominent lips. (Fig. 1, A–D) She had moderate pectus excavatum, bilateral winging of the scapula and mild left lumbar prominence upon forward bending. Her muscle tone, strength and reflexes were normal. She had numerous hyperpigmented nevi, but no deep palmar creases.

Noonan syndrome was suspected and mutation analysis was performed clinically through a panel approach. A novel HRAS mutation (c.179G>A; p.Gly60Asp) was identified. No sequence change was identified in *BRAF, CBL, KRAS, MAP2K1, MAP2K2, NRAS, PTPN11, SHOC2* and *SOS1*. An informative SNP (rs12628) was used to determine parental origin of the germline mutation by allele specific amplification.

Individual 2 (CS#442)—This male patient was born after an uneventful pregnancy without prenatal exposures and with normal prenatal ultrasound examinations. His mother was a healthy 39-year-old and his father was 38 years old. They had a previous first trimester loss and a healthy daughter. A paternal half-sister was in good health. Both parents were of Cuban ancestry, but not known to be consanguineous. The patient was born and received medical care until age 2 11/12 years in Cuba, resulting in limited availability of medical records.

Delivery occurred at 39 weeks gestation by repeat cesarian after spontaneous onset of labor. Birth weight was 3.9 kg (90th centile); birth length and OFC were not recalled. While no resuscitation was necessary, he required a 15 day hospitalization for “blue episodes”

ultimately attributed to a transient cardiac arrhythmia. The arrhythmia was reportedly characterized by episodes of tachycardia and bradycardia, but the specific diagnosis was unknown to his parents. It resolved after two weeks of treatment with an unspecified medication. Thereafter, he was considered a healthy infant. He had no difficulties with latching, sucking or swallowing but he was treated for gastro-esophageal reflux.

The patient reportedly had normal gross motor milestones in infancy, but hypotonia was noted and delays in fine motor skills, language acquisition and social skills were identified. He was in a special education class with an individualized education program. He was diagnosed with attention deficit hyperactivity disorder and oppositional defiant disorder with symptom improvement on medication. While he produced sweat normally, he had a tendency to become flushed and feel warm in environments considered comfortable by others, and he scratched his skin frequently without apparent reason.

Cardiac evaluations including Holter monitoring and echocardiogram performed at age 8 years had normal results.

At age 8 years his height was 122 cm (5th centile), weight 23 kg (5–10th centile) and OFC 55.8 cm (just above 98th centile). High anterior hair line and tall forehead were noted and facial features are shown in Fig. 1(E–G). Pertinent positive findings on physical examination included a collection of small tag-like skin papules involving the right areola and chest medial to the right nipple, reportedly unchanged over time. Significant hyperextensibility of the small joints of the hands were noted. He had low muscle tone and poor coordination.

A chromosomal microarray analysis had normal results. Noonan syndrome was suspected and mutation analysis was performed clinically through a panel approach. A de novo *HRAS* mutation (c.179G>A; p.Gly60Asp) was identified. An informative SNP (rs41258054) was subsequently used to determine parental origin of the germline mutation (supplemental Fig. 2).

In addition, a maternally derived *SHOC2* sequence change (c.1490 C>A; p.Thr497Lys) was seen. No sequence change was identified in *BRAF, CBL, KRAS, MAP2K1 MAP2K2, NRAS, PTPN11, RAF1* and *SOS1.*

Individual 3 (CS#451)—This male patient was born at term by cesarian for fetal distress after a pregnancy with reported polyhydramnios. He was the first child for his parents who were non-consanguineous. His birth weight was 4.25 kg (90–97th centile), length 48.3 cm (10th centile), OFC not documented. A cardiac murmur noted at age 2 weeks resulted in cardiac echography, which showed a thickened dysplastic pulmonic valve causing mild pulmonic stenosis. A mildly thickened left ventricular myocardium was seen. He had gastro-esophageal reflux resulting in emesis until age 3 months without other feeding difficulties or failure-to-thrive. A cranial CT scan performed due to a concern for craniosynostosis showed an arachnoid cyst with mild anterior displacement of the left cerebellar hemisphere. His development was age appropriate with walking independently at age 10 months.

At age 13 months his weight was 8.9 kg (5th centile), length 76.3 cm (50th centile) and OFC 48.5 cm (90th centile). Facial findings included telecanthus and ptosis (Fig. 2A, B), a long

and prominent philtrum and slightly thickened helices. His physical findings were otherwise unremarkable.

Noonan syndrome was suspected and mutation analysis performed clinically through a panel approach. The *HRAS* mutation (c.179G>A; p.Gly60Asp) was identified. No sequence change was identified in *BRAF, CBL, KRAS, MAP2K1 MAP2K2, NRAS, PTPN11, SHOC2* and *SOS1*.

Individual 4—Individual 4 is Individual 3's mother. Her medical history was notable for mild problems with reading but graduated from high school without requiring resource classes. She did not have failure-to-thrive or short stature (Table I).

She had slightly thick and curly hair, deep blue eyes, an inverted triangle shaped face with pronounced nasolabial folds and a relatively wide mouth (Fig. 2, C, D). In addition to several raised skin lesions on her face she had a growth on the inner surface of her lower lip (Fig. 2, E). Her feet showed callouses and deep plantar creases (Fig. 2F, G).

Based on her facial features, deep plantar creases and history of learning differences, she was thought likely to carry the familial sequence change. Molecular testing was performed from a cheek swab derived DNA sample on a research basis with informed research consent. She was heterozygous for the *HRAS* mutation (c.179G>A).

Functional Studies

Plasmid Construction—We amplified the coding region of wild-type *HRAS* for the generation of an expression construct by using *HRAS*-specific PCR primers and *HRAS* cDNA as a template. Mutated *HRAS* cDNA inserts [c.35G>T (p.Gly12Val), c.50G>A (p.Ser17Asn) and c.179G>A (p.Gly60Asp)] were established by PCR-mediated mutagenesis. Purified PCR products were cloned into pENTR/D-TOPO (Invitrogen, Karlsruhe, Germany) according to the provided protocol. Constructs were sequenced for integrity and used for subcloning wild-type and mutated HRAS coding regions into plasmid pMT2SM-HA-DEST (N-terminal HA epitope). $NF1^{333}$ in pcDNA3-FLAG contains residues 1198–1530 of human NF1 comprising the functional GAP-related domain that is able to bind to wild-type HRAS and stimulate GTP hydrolysis.

Cell Culture and Transfection—COS-7 and HEK293 cells were cultured in Dulbecco's Modified Eagle Medium (DMEM; Invitrogen) containing 10% serum (Invitrogen) and penicillin-streptomycin (100 U/ml and 100 mg/ml, respectively) (Invitrogen) at 37°C and 5% CO_2. Transfections were performed using Lipofectamine 2000 Reagent (Invitrogen) according to the manufacturer's protocol. For EGF stimulation, cells were blocked overnight by serum starvation (0.1% serum), followed by incubation in DMEM containing 10 ng/ml EGF (Sigma, Taufkirchen, Germany).

RAS Pull-down Assay—The RAS-binding domain (RBD) of RAF1 (amino acids 51-131), the RBD of PI3K (PIK3CA) (amino acids 127-314), the RAS-association (RA) domain of RALGDS (amino acids 777–872) and the RA domain of PLC1 (PLCE1) (amino acids 2130–2240) were used to specifically precipitate GTP-bound RAS proteins from cell

extracts. Preparation of GST-RBD/RA beads, cell lysis and precipitation of GTP-bound RAS were described elsewhere [Rosenberger et al., 2009]. After SDS PAGE and transfer to polyvinylidene difluorid (PVDF) membranes, total and precipitated (active) HA-tagged HRAS was detected using peroxidase-conjugated rat monoclonal anti-HA antibody (Roche, Mannheim, Germany; clone 3F10; 1:5000 dilution). For loading control, membranes were incubated with mouse anti-glyceraldehyde-3-phosphate dehydrogenase (GAPDH) (Abcam, Cambridge, UK; no. ab8245, 1:5000 dilution), followed by peroxidase-coupled secondary anti-mouse antibody (Amersham Pharmacia Biotech, Freiburg, Germany; no. NA9310; 1:8000 dilution).

Co-immunoprecipitation—Transiently transfected COS-7 cells were lyzed in ice-cold cell lysis buffer [150 mM Tris-HCl, pH 8.0; 50 mM NaCl; 1 mM EDTA; 0.5% Nonidet P-40; complete Mini Protease Inhibitors (Roche); 0.7 mg/ml Pepstatin] and cell extracts were clarified by centrifugation. The supernatants were transferred to 40 ml EZview™ Red Anti-HA Affinity Gel (Sigma) and incubated for 2 hours at 4°C on a rotator. Precipitates were collected by repeated centrifugation and washing with cell lysis buffer, re-suspended in sample buffer (33% glycerol; 80 mM Tris-HCl, pH 6.8; 0.3 M Dithiothreitol; 6.7% sodium dodecyl sulphate; 0.1% bromophenol blue) and subjected to SDS PAGE and immunoblotting.

Immunoblotting—Twenty-four hours after transfection, cells were cultured as specified, then washed with PBS and scraped off in modified radioimmunoprecipitation assay buffer [50 mM Tris–HCl, pH 8.0; 150 mMNaCl; 1% Nonidet P-40; 0.5% sodiumdeoxycholate; 0.1% SDS; 1 mM phenylmethylsulfonyl fluoride; 1 mM Na3VO4; 10 mM NaF; 1 Complete Mini protein inhibitor cocktail tablet (Roche) per 10 ml]. Cellular biochemical reactions were stopped by freezing lysates in liquid nitrogen. After thawing on ice, cell debris was removed, solutions were supplemented with sample buffer, and proteins were separated on SDS-polyacrylamide gels and transferred to PVDF membranes. Following blocking (20 mM Tris-HCl, pH 7.4; 150 mM NaCl; 0.1% Tween-20; 4% non-fat dry milk) and washing (20 mM Tris-HCl, pH 7.4; 150 mM NaCl; 0.1% Tween-20), membranes were incubated in primary antibody solution (20 mM Tris-HCl, pH 7.4; 150 mM NaCl; 0.1% Tween-20; 5% BSA or 0.5% non-fat dry milk) containing the appropriate antibodies. Rabbit polyclonal antibodies against MEK1/2 (Cell Signaling Tech., Danvers, MA, USA; no. 9122; 1:1000 dilution), phospho-MEK1/2 (Ser217/221) (Cell Signaling Tech.; no. 9121; 1:1000 dilution), p44/42 MAP kinase (ERK1/2) (Cell Signaling Tech.; no. 9102, 1:1000 dilution), phospho-p44/42 MAP kinase (ERK1/2) (Thr202/Tyr204) (Cell Signaling Tech.; no. 9101, 1:1000 dilution), Akt1/2/3 (Cell Signaling Tech.; no. 9272; 1:1000 dilution), and phospho-Akt1/2/3 (Ser473) (Cell Signaling Tech.; no. 9271; 1:1000 dilution) were used. Membranes were washed and incubated with peroxidase-coupled secondary anti-rabbit antibody (Amersham Pharmacia Biotech; no. NA9340V; 1:8000 dilution). After final washing, immunoreactive proteins were visualized using the Immobilon Western Chemiluminescent HRP Substrate (Millipore, Schwalbach, Germany).

RESULTS

A novel HRAS mutation, HRAS c.179G>A (p.Gly60Asp), was identified through clinical testing in individuals with a suspected rasopathy. This mutation occurred de novo in Individuals 1 and 2 and was maternally transmitted in Individual 3. Allele specific amplification (ASA) revealed a paternal origin of the mutation in Individuals 1 and 2 (Supplemental Fig. 2).

Glycine 60 in HRAS is highly conserved among RAS paralogs and HRAS orthologs (data not shown). It is part of the HRAS switch II domain (amino acids 59-67) that mediates binding of HRAS with various regulator and effector proteins (Fig. 3A) [Boriack-Sjodin et al., 1998; Polakis and McCormick, 1993; Scheffzek et al., 1997; Stieglitz et al., 2008; Vetter and Wittinghofer, 2001]. Of note, disease-associated mutations of the homologous amino acid in KRAS (p.Gly60Arg) and NRAS (p.Gly60Glu) have been shown to exert strong impact on RAS function [Gremer, 2010b; Cirstea et al., 2010; Runtuwene et al., 2011; Tyner et al., 2009], thus we aimed to complete functional studies by characterizing the consequences of the HRAS p.Gly60Asp mutation.

HRAS p.Gly60Asp Strongly Co-precipitates with its Effector Protein RAF1

To explore the molecular consequences of the p.Gly60Asp mutation, we transiently transfected COS-7 cells with various hemagglutinin (HA)-tagged *HRAS* constructs. To uncover alterations linked to specific cell environments we cultured cells under different conditions, including serum starvation (0.1% serum), normal growth conditions (10% serum), and EGF stimulation (0.1% serum → EGF-stimulation) (Fig. 3B). We precipitated HRAS protein variants from COS-7 cell extracts by using glutathione S-transferase (GST)-fusion protein of the RAS-binding domain (RBD) of RAS effector protein RAF1 (RAF1[RBD]). We could efficiently pull down constitutively active HA-HRAS^{Gly12Val}, but not the dominant negative mutant HA-HRAS^{Ser17Asn} [Farnsworth and Feig, 1991; Stacey et al., 1991] from cell extracts under all tested conditions (Fig. 3B, pcpt). The amount of HA-HRAS^{Gly60Asp} in the precipitates was clearly elevated compared to active HA-HRAS^{WT} under these culture conditions (Fig. 3B, pcpt); however, it was decreased compared to HA-HRAS^{Gly12Val} (Fig. 3B, pcpt). These data suggest that independent of cellular growth conditions, HA-HRAS^{Gly60Asp} forms stable complexes with its effector RAF1. Of note, these experiments do not allow us to discriminate if increased binding to RAF1 is due to accumulation of HRAS^{Gly60Asp} in the active conformation or due to an altered structure of the HRAS^{Gly60Asp} switch II region.

p.Gly60Asp Does Not Alter Binding to RAS Effectors PIK3CA, RALGDS and PLCE1

We evaluated binding properties of HRAS^{Gly60Asp} to additional signaling effectors. HA-HRAS variants were overexpressed in COS-7 cells, and, following starvation, cells were stimulated with EGF. Activated HRAS proteins were precipitated from cell extracts using the RAS-binding domain (RBD) of PIK3CA, the RAS association (RA) domain of PLCE1 or the RA domain of RALGDS (Fig. 3C). As expected, we could efficiently pull down HA-HRAS^{Gly12Val} but not HA-HRAS^{Ser17Asn} from cell extracts with all tested effector domains (Fig. 3C, pcpt). In contrast, the amount of precipitated HA-HRAS^{Gly60Asp} was similar to

$HRAS^{WT}$ (Fig. 3C, pcpt). Taken together, binding of $HRAS^{Gly60Asp}$ to three downstream effectors, PIK3CA, PLCE1 and RALGDS, was normal in these experiments, thus providing no evidence for altered binding to these effectors or for accumulation of $HRAS^{Gly60Asp}$ in the GTP-bound state.

p.Gly60Asp Does Not Affect HRAS Interaction with NF1 GAP

HRAS has low intrinsic GTPase activity that is dramatically stimulated by GAPs, and the switch II region is critical for binding active HRAS with GAP proteins [Ahmadian et al., 2003; Scheffzek et al., 1997; Scheffzek et al., 1998]. To analyze binding between HRAS and the RAS-specific NF1 GAP, we co-expressed the GAP-related domain of NF1, called $NF1^{333}$, together with HRAS protein variants in COS-7 cells and performed co-immunoprecipitation. We pulled down FLAG-$NF1^{333}$ together with HA-$HRAS^{WT}$, most likely reflecting the fraction of active HA-$HRAS^{WT}$ molecules in the cell lysates (Fig. 4). Consistently, FLAG-tagged $NF1^{333}$ strongly co-precipitated with constitutively active HA-$HRAS^{Gly12Val}$, but only very weakly with dominant negative HA-$HRAS^{Ser17Asn}$ (Fig. 4). Interestingly, despite amino acid 60's location within the switch II region, FLAG-$NF1^{333}$ co-precipitated with HA-$HRAS^{Gly60Asp}$ (Fig. 4) indicating that substitution of HRAS Gly^{60} by Asp does not interfere with NF1 GAP binding. Moreover, co-precipitation was not elevated compared with HA-$HRAS^{WT}$, which functionally clearly distinguishes $HRAS^{Gly60Asp}$ from $HRAS^{Gly12Val}$ and suggests that $HRAS^{Gly60Asp}$ is not hyperactive.

HRAS p.Gly60Asp Does Not Increase RAF-MAPK and PI3K-AKT Signaling Pathway Activation

To gain insight into the effects of the p.Gly60Asp change on HRAS downstream signal flux, we measured levels of phosphorylated MEK1/2, ERK1/2 and AKT in COS-7 cells ectopically expressing HA-tagged HRAS protein variants. HA-$HRAS^{Gly12Val}$ promoted enhanced MEK1/2, ERK1/2 and AKT phosphorylation under serum-starved (Fig. 5, 0.1% serum) and basal (Fig. 5, 10% serum) conditions, as well as upon EGF stimulation (Fig. 5, 0.1%serum→EGF stimulation). Expectedly, the dominant negative mutant HA-$HRAS^{Ser17Asn}$ induced only a very weak signaling response (Fig. 5). Surprisingly, cells expressing HA-$HRAS^{Gly60Asp}$ showed similar or even decreased MEK1/2, ERK1/2 and AKT phosphorylation compared to HA-$HRAS^{WT}$ under all tested culture conditions (Fig. 5). We successfully reproduced these results using an alternate cell line, HEK293 (data not shown). Together, these data indicate that the HRAS p.Gly60Asp mutation does not result in intensified mitogen-activated protein kinase (MAPK) or PI3K-AKT signal transduction.

DISCUSSION

We report four Individuals with a novel *HRAS* mutation predicting a p.Gly60Asp amino acid substitution. Identification of these Individuals became possible through a test panel approach applied due to a clinical diagnosis of Noonan syndrome. The test panel surprisingly revealed a heterozygous missense change in *HRAS,* suggesting a molecular diagnosis of Costello syndrome. The novel SHOC2 p.Thr497Lys in Individual 2 was considered non-pathogenic based on its inheritance from a clinically unaffected mother, mutation prediction program results (PROVEAN: neutral; SIFT: tolerated), and the specific

functional effect of the only known pathogenic SHOC2 mutation which invariably occurs as p.Ser2Gly.

Phenotype

The Individuals' physical and developmental phenotype is less severe than that associated with the most common Costello syndrome causing *HRAS* mutation, p.Gly12Ser (Table I). However, each finding is consistent with a diagnosis of Costello syndrome, for example the atrial tachycardia requiring medication in Individuals 1 and 2 may represent the multifocal atrial tachycardia typical of Costello syndrome, and pulmonic stenosis occurs in 20% of patients [Lin et al., 2011]. Nystagmus and cerebellar tonsillar ectopy with crowding of the posterior fossa have been reported in Costello syndrome [Gripp et al., 2010].

The absence of failure-to-thrive, short stature, severe hypertrophic cardiomyopathy and malignant tumors in the individuals reported here is notably different from the typical Costello syndrome phenotype. A comparable attenuated Costello syndrome phenotype has been reported for the HRAS p.Thr58Ile mutation [Gripp et al., 2008; Gripp et al., 2012a] (Table I). Facial features in Individuals 1–4 (Fig. 1, 2) include a tall forehead with mild bitemporal narrowing in childhood (1A, 2A, B), changing to an inverted triangle shape in older individuals (1C; 2C). Curly hair is present in Individuals 1, 2, and 3. Individual 1 has a wide mouth (2C), and Individual 4 has an intraoral lesion that may represent a papilloma. While these facial features are consistent with a rasopathy, they are less coarse or distinctive than those seen in Costello syndrome resulting for the common HRAS p.Gly12Ser mutation, and more in keeping with findings typically seen in Noonan syndrome.

While no formal cognitive testing was completed, the normal school performance in Individual 1 and the normal functioning of Individual 4 despite learning differences suggest a level of functioning higher than that of typical Costello syndrome patients. Overall, the phenotypic presentation of the Individuals reported here may be best described as attenuated Costello syndrome, similar to that previously reported for HRAS p.Thr58Ile and p.Ala146Val [Gripp et al., 2008]. Notably, the serious clinical manifestation in a patient with lethal HCM due to a mutation predicting KRAS p.Gly60Asp underlines the biological differences between HRAS and KRAS [Nosan et al. 2013].

Genotype

The *HRAS* c.179G>A mutation occurred de novo in Individuals 1 and 2 and was maternally transmitted in Individual 3. The paternal origin in Individuals 1 and 2 was determined using allelic specific amplification (ASA). The paternal mutation origin is consistent with almost exclusively paternal origin for de novo *HRAS* mutations [Sol-Church et al., 2006; Giannoulatou et al., 2013]. Transmission from a parent with apparent heterozygosity for an *HRAS* mutation has been reported only once, for the p.Thr58Ile amino acid change associated with an attenuated phenotype [Gripp et al., 2012a]. In contrast, transmission of the common p.Gly12Ser mutation has been reported exclusively from a parent with somatic or presumed gonadal mosaicism [Sol-Church et al., 2009; Gripp et al., 2011b].

Somatic HRAS mutations

Missense mutations in the proto-oncogene *HRAS* occur as somatic changes in solid tumors and the transforming potential of different mutations has been studied extensively. The Cosmic database does not list a missense mutation affecting amino acid 60 in a tumor. This contrasts sharply with amino acid 61 in which numerous missense changes were identified, indicating high transforming potential of these changes [Sanger Institute, Cosmic].

Functional effects of HRAS p.Gly60Asp

Here, we provide evidence for an unusual consequence of a Costello syndrome associated HRAS mutation: the p.Gly60Asp change results in enhanced binding with RAF1, but not with PIK3CA, PLCE1 or RALGDS; however augmented RAF binding is not transduced into hyperactivation of the RAF-MAPK downstream signaling cascade.

In line with increased binding of $HRAS^{Gly60Asp}$ to RAF1 peptide (Fig. 3B), Noonan syndrome-associated amino acid change p.Gly60Glu in NRAS also resulted in enhanced co-precipitation with RAF1 peptide. Therefore, $NRAS^{Gly60Glu}$ has been suggested to be locked in a hyperactive state [Runtuwene et al., 2011; Tyner et al., 2009; Cirstea et al., 2010]. In contrast to our results, ectopic expression of $NRAS^{Gly60Glu}$ in COS-7 or HEK293 cells induced enhanced MAPK downstream signaling [Runtuwene et al., 2011; Tyner et al., 2009; Cirstea et al., 2010]. The molecular consequences become even more puzzling when considering functional data for the KRAS p.Gly60Arg change described in patients with rasopathies [Niihori et al., 2006; Zenker et al. 2007; Kratz et al., 2009]. Although binding affinity of $KRAS^{Gly60Arg}$ with RAF1 (and also RALGDS) was strongly impaired, ectopically expressed $KRAS^{Gly60Arg}$ efficiently co-precipitated with RAF1 effector peptide and induced elevated MAPK signaling in COS-7 cells under serum-free conditions [Gremer et al., 2010b]. It was suggested that accumulation of $KRAS^{Gly60Arg}$ in the GTP-bound state due to profound GAP insensitivity is compensated by a strongly reduced effector interaction [Gremer et al., 2010b]. In fact, RAS effectors and RAS GAPs share an overlapping interactive region on RAS, including switch II [Vetter and Wittinghofer, 2001]. The residual binding capacity of activated $KRAS^{Gly60Arg}$ in combination with RAF1 resulted in a moderately enhanced MAPK downstream signal transduction [Gremer et al., 2010b]. However, no significant stimulation of ELK transcription, a downstream consequence of MAPK signaling, has been observed in NIH 3T3 cells overexpressing $KRAS^{Gly60Arg}$ [Niihori et al., 2006]. We did not detect enhanced signal flux, neither in the MAPK nor in the AKT signaling cascade. Viewed together, data about the functional consequences of disease-associated RAS amino acid 60 changes ($HRAS^{Gly60Asp}$, $NRAS^{Gly60Glu}$, $KRAS^{Gly60Arg}$) are not consistent, which might be due to protein isoform specific molecular features, or simply to the nature of the substituted amino acid. The functional importance of RAS amino acid 60 is evident, because in the active GTP-bound RAS conformation two hydrogen bonds extend from γ-phosphate oxygens to the main-chain NH groups of the invariant glycine 60 and threonine 35 in switch II and I, respectively. This state can be described as a loaded-spring conformation before release of the γ-phosphate through GTP hydrolysis triggers the switch regions' relaxation into the GDP-specific conformation [Vetter and Wittinghofer, 2001]. Previously, the molecular consequences of the change from glycine 60 to alanine in HRAS have been characterized in detail and p.Gly60Ala was shown to

inhibit the ability of viral HRAS to transform NIH 3T3 cells and to activate its downstream effector Raf-1. Moreover, the mutant was unable to induce germinal vesicle breakdown in Xenopus oocytes, which is a surrogate marker for the mutagenic potential of RAS variants [Sung et al., 1995; Sung et al., 1996; Hwang et al., 1996]. Thus, $RAS^{Gly60Ala}$ was classified as a dominant negative mutant. Various molecular deficits have been demonstrated for HRAS p.Gly60Ala including accumulation in the GTP-bound state, decreased GTPase activity, reduced effector binding and the formation of abnormally stable complexes with GEF proteins [Sung et al., 1995; Sung et al., 1996; Hwang et al., 1996; Ford et al., 2005]. Based on these data, two hypotheses for the dominant negative effect of $HRAS^{Gly60Ala}$ have been suggested. First, $HRAS^{Gly60Ala}$ sequesters endogenous downstream effectors including RAF1 kinase into inactive complexes [Sung et al., 1996], and second, $HRAS^{Gly60Ala}$ sequesters GEF proteins in non-productive complexes [Ford et al., 2005]. Regardless of which is the main molecular mechanism, its result would be a constriction in RAS-dependent signaling pathways. Perfectly in line with this, we show here that activation of MEK1/2 was decreased in $HRAS^{Gly60Asp}$ expressing cells compared to cells expressing $HRAS^{WT}$. Notably, RAF1 binding was increased in our assays, thus sequestration of endogenous RAF1 in non-productive signaling complexes may contribute (non-exclusively) to a dominant negative effect of $HRAS^{Gly60Asp}$. However, this hypothesis remains to be proven.

Considering that enhanced RAS-MAPK signaling is thought to be the primary cause of RASopathies, our results are highly unexpected. How can we explain an obvious rasopathy phenotype without the obligate proof of hyperactivated RAS-dependent signaling? The answer has been given previously: impaired reactivity to stimuli resulting in reduced and disrupted capacity to transduce incoming signals to downstream effectors is a harmful consequence of HRAS/rasopathy-associated mutations [Lorenz et al., 2013]. In principle, constitutive HRAS activation and hyperactivation of HRAS-dependent signaling paths due to any Costello syndrome-associated mutation can alternatively be interpreted as reduced reagibility to stimuli [Lorenz et al., 2013]. From this novel viewpoint, $HRAS^{Gly60Asp}$ may be unable to transmit incoming signals due to the formation of non-productive signaling complexes. Similarly, a germline HRAS alteration (c.266C>G; p.Ser89Cys) resulting in decreased HRAS downstream signaling was reported in siblings with clinical features reminiscent of Costello syndrome [Gripp et al., 2012b]. Furthermore, based on experiments with primary fibroblasts of patients with Costello syndrome, altered cellular response to growth factors rather than constitutive activation of HRAS downstream signaling molecules may contribute to the phenotype [Rosenberger et al., 2009]. This hypothesis is corroborated by the analysis of an $HRAS^{WT/Gly12Val}$ mouse model for Costello syndrome showing normal phosphorylation levels of Erk, Mek and Akt in all tissues tested [Schuhmacher et al., 2008]. In conclusion, the attenuated phenotype in these individuals with a novel HRAS mutation further supports strong genotype-phenotype correlations for germline HRAS mutations. Simultaneously, its overlap with Noonan syndrome further illustrates the rasopathies' shared findings and supports the use of molecular panel testing. Additional clinical studies are needed in order to determine specific mutation specific risks, such as malignancy and hypertrophic cardiomyopathy. Our functional data provide evidence for an attenuating effect of a RASopathy-associated mutation on RAS-dependent downstream signaling and thereby,

shift the focus from harmful HRAS hyperactivation toward reduced reagibility/reactivity as a critical pathomechanism for rasopathies. Our data also have important implications on future treatment strategies because the application of RAS signaling inhibitors to block hyperactivated signaling pathways may not restitute the cells reagibility/reactivity to stimuli.

Genebank Reference Sequences

HRAS (HRAS, H-Ras) NM_005343.2, NM_176795.3; *MAP2K1/MAP2K2* (MEK1/2) NM_002755.3/NM_030662.2; *MAPK3/MAPK1* (ERK1/2) NM_002745.4/NM_001040056.1; *AKT1/AKT2/AKT3* (AKT1-3) NM_001014431.1/NM_001626.3/NM_005465.3; *GAPDH* (GAPDH) NM_002046.3; *RAF1* (CRAF, c-Raf) NM_002880.3; *RALGDS* (RalGDS, RalGEF) NM_006266.2; *PIK3CA* (PI3Ka, p110-alpha) NM_006218.2; *PLCE1* (PLC1, PLC11) NM_016341.3; *NF1* (NF1, neurofibromin 1) NM_001042492. Protein names are denoted in parentheses.

Acknowledgments

We thank the Individuals and their families for allowing us to share this information. We thank Bradley Williams, GC from GeneDx for his help in identifying Individual 2. This report was supported by The Nemours Foundation and by funds to KSC from NIH-NIGMS grants P20GM103464 and grant P20GM103446 instrumentation core programs, the University of Utah Clinical Genetics Research Program: Phenotyping Core (CGRP), and the National Center for Research Resources and the National Center for Advancing Translational Sciences, National Institutes of Health, through Grant UL1RR025764.

References

Ahmadian MR, Kiel C, Stege P, Scheffzek K. Structural fingerprints of the Ras-GTPase activating proteins neurofibromin and p120GAP. J Mol Biology. 2003; 329:699–710.

Aoki Y, Niihori T, Kawame H, Kurosawa K, Ohashi H, Tanaka Y, Filocamo M, Kato K, Suzuki Y, Kure S, Matsubara Y. Germline mutations in HRAS proto-oncogene cause Costello syndrome. Nat Genet. 2005; 37:1038–1040. [PubMed: 16170316]

Boriack-Sjodin PA, Margarit SM, Bar-Sagi D, Kuriyan J. The structural basis of the activation of Ras by Sos. Nature. 1998; 394:337–343. [PubMed: 9690470]

Cirstea IC, Kutsche K, Dvorsky R, Gremer L, Carta C, Horn D, Roberts AE, Lepri F, Merbitz-Zahradnik T, Konig R, Kratz CP, Pantaleoni F, Dentici ML, Joshi VA, Kucherlapati RS, Mazzanti L, Mundlos S, Patton MA, Silengo MC, Rossi C, Zampino G, Digilio C, Stuppia L, Seemanova E, Pennacchio LA, Gelb BD, Dallapiccola B, Wittinghofer A, Ahmadian MR, Tartaglia M, Zenker M. A restricted spectrum of NRAS mutations causes Noonan syndrome. Nat Genet. 2010; 42:27–29. [PubMed: 19966803]

Denayer E, Parret A, Chmara M, Schubbert S, Vogels A, Devriendt K, Frijns JP, Rybin V, de Ravel TJ, Shannon K, Cools J, Scheffzek K, Legius E. Mutation analysis in Costello syndrome: functional and structural characterization of the HRAS p.Lys117Arg mutation. Hum Mutat. 2008; 29:232–239. [PubMed: 17979197]

Farnsworth CL, Feig LA. Dominant inhibitory mutations in the Mg(2+)-binding site of RasH prevent its activation by GTP. Mol Cell Biology. 1991; 11:4822–4829.

Fasano O, Aldrich T, Tamanoi F, Taparowsky E, Furth M, Wigler M. Analysis of the transforming potential of the human H-ras gene by random mutagenesis. Proc Natl Acad Sci USA. 1984; 81:4008–4012. [PubMed: 6330729]

Ford B, Skowronek K, Boykevisch S, Bar-Sagi D, Nassar N. Structure of the G60A mutant of Ras: implications for the dominant negative effect. J Biol Chem. 2005; 280:25697–25705. [PubMed: 15878843]

Giannoulatou E, McVean G, Taylor IB, McGowan SJ, Maher GJ, Iqbal Z, Pfeifer SP, Turner I, Burkitt Wright EM, Shorto J, Itani A, Turner K, Gregory L, Buck D, Rajpert-De Meyts E, Looijenga LH,

Kerr B, Wilkie AO, Goriely A. Contributions of intrinsic mutation rate and selfish selection to levels of de novo HRAS mutations in the paternal germline. Proc Natl Acad Sci USA. 2013; 110:20152–20157. [PubMed: 24259709]

Gideon P, John J, Frech M, Lautwein A, Clark R, Scheffler JE, Wittinghofer A. Mutational and kinetic analyses of the GTPase-activating protein (GAP)-p21 interaction: the C-terminal domain of GAP is not sufficient for full activity. Mol Cell Biology. 1992; 12:2050–2056.

Gremer L, De Luca A, Merbitz-Zahradnik T, Dallapiccola B, Morlot S, Tartaglia M, Kutsche K, Ahmadian MR, Rosenberger G. Duplication of Glu37 in the switch I region of HRAS impairs effector/GAP binding and underlies Costello syndrome by promoting enhanced growth factor-dependent MAPK and AKT activation. Hum Mol Genet. 2010a; 19:790–802. [PubMed: 19995790]

Gremer L, Merbitz-Zahradnik T, Dvorsky R, Cirstea IC, Kratz CP, Zenker M, Wittinghofer A, Ahmadian MR. Germline KRAS mutations cause aberrant biochemical and physical properties leading to developmental disorders. Hum Mutat. 2010b; 32:33–43. [PubMed: 20949621]

Gripp KW, Bifeld E, Stabley DL, Hopkins E, Meien S, Vinette K, Sol-Church K, Rosenberger G. A novel HRAS substitution (c.266C>G; p.S89C) resulting in decreased downstream signaling suggests a new dimension of RAS pathway dysregulation in human development. Am J Med Genet Part A. 2012b; 158A:2106–2118. [PubMed: 22821884]

Gripp KW, Hopkins E, Doyle D, Dobyns WB. High incidence of progressive postnatal cerebellar enlargement in Costello syndrome: Brain overgrowth associated with HRAS mutations as the likely cause of structural brain and spinal cord abnormalities. Am J Med Genet Part A. 2010; 152A:1161–1168. [PubMed: 20425820]

Gripp KW, Hopkins E, Serrano A, Leonard NJ, Stabley DL, Sol-Church K. Transmission of the rare HRAS mutation (c. 173C>T; p.T58I) further illustrates its attenuated phenotype. Am J Med Genet Part A. 2012a; 158A:1095–1101. [PubMed: 22488832]

Gripp KW, Hopkins E, Sol-Church K, Stabley DL, Axelrad ME, Doyle D, Dobyns WB, Hudson C, Johnson J, Tenconi R, Graham GE, Sousa AB, Heller R, Piccione M, Corsello G, Herman GE, Tartaglia M, Lin AE. Phenotypic analysis of individuals with Costello syndrome due to HRAS p.G13C. Am J Med Genet Part A. 2011a; 155A:706–716. [PubMed: 21438134]

Gripp KW, Innes MA, Axelrad ME, Gillan TL, Parboosingh JS, Davies C, Leonard NJ, Lapointe M, Doyle D, Catalano S, Nicholson L, Stabley DL, Sol-Church K. Costello syndrome associated with novel germline HRAS mutations: An attenuated phenotype? Am J Med Genet. 2008; 146A:683–690. [PubMed: 18247425]

Gripp, KW.; Lin, AE. Costello Syndrome 2006 Aug 29. In: Pagon, RA.; Adam, MP.; Bird, TD., et al., editors. GeneReviews® [Internet]. Seattle (WA): University of Washington, Seattle; 1993–2014. Updated 2012 Jan 12Available from: http://www.ncbi.nlm.nih.gov/books/NBK1507/

Gripp KW, Lin AE. Costello Syndrome: A Ras/MAPK pathway syndrome (Rasopathy) resulting from HRAS germline mutations. Genet Med. 2012; 14:285–292. [PubMed: 22261753]

Gripp KW, Lin AE, Stabley DL, Nicholson L, Scott CI Jr, Doyle D, Aoki Y, Matsubara Y, Zackai EH, Lapunzina P, Gonzalez-Meneses A, Holbrook J, Agresta CA, Gonzalez IL, Sol-Church K. HRAS mutation analysis in Costello syndrome: genotype and phenotype correlation. Am J Med Genet A. 2006; 140:1–7. [PubMed: 16329078]

Gripp KW, Stabley DL, Geller PL, Hopkins E, Stevenson DA, Carey JC, Sol-Church K. Molecular confirmation of HRAS p.G12S in siblings with Costello syndrome. Am J Med Genet Part A. 2011b; 155:2263–2268. [PubMed: 21834037]

Guo Z, Ahmadian MR, Goody RS. Guanine nucleotide exchange factors operate by a simple allosteric competitive mechanism. Biochemistry. 2005; 44:15423–15429. [PubMed: 16300389]

Hwang MCC, Sung YJ, Hwang YW. The differential effects of the Gly-60 to Ala mutation on the interaction of H-Ras p21 with different downstream targets. J Biol Chem. 1996; 271:8196–8202. [PubMed: 8626511]

Karnoub AE, Weinberg RA. Ras oncogenes: split personalities. Nat Rev Mol Cell Biol. 2008; 9:517–531. [PubMed: 18568040]

Kerr B, Delrue MA, Sigaudy S, Perveen R, Marche M, Burgelin I, Stef M, Tang B, Eden OB, O'Sullivan J, De Sandre-Giovannoli A, Reardon W, Brewer C, Bennett C, Quarell O, M'Cann E,

Donnai D, Stewart F, Hennekam R, Cave H, Verloes A, Philip N, Lacombe D, Levy N, Arveiler B, Black G. Genotype-phenotype correlation in Costello syndrome: HRAS mutation analysis in 43 cases. J Med Genet. 2006; 43:401–405. [PubMed: 16443854]

Kratz CP, Zampino G, Kriek M, Kant SG, Leoni C, Pantaleoni F, Oudesluys-Murphy AM, di Rocco C, Kloska SP, Tartaglia M, Zenker M. Craniosynostosis in patients with Noonan syndrome caused by germline KRAS mutations. Am J Med Genet Part A. 2009; 149A:1036–1040. [PubMed: 19396835]

Lin AE, Alexander ME, Colan SD, Kerr B, Rauen KA, Noonan J, Baffa J, Hopkins E, Sol-Church K, Limongelli G, Digilio MC, Marino B, Innes AM, Aoki Y, Silberbach M, Delrue MA, White SM, Hamilton RM, O'Connor W, Grossfeld PD, Smoot LB, Padera RF, Gripp KW. Clinical, pathological, and molecular analyses of cardiovascular abnormalities in Costello syndrome: A Ras/MAPK pathway syndrome. Am J Med Genet Part A. 2011; 155:1–22.

Lo IFM, Brewer C, Shannon N, Shorto J, Tang B, Black G, Soo MT, Ng DKK, Lam STS, Kerr B. Severe neonatal manifestations of Costello syndrome. J Med Genet. 2008; 45:167–171. [PubMed: 18039947]

Lorenz S, Lissewski C, Simsek-Kiper PO, Alanay Y, Boduroglu K, Zenker M, Rosenberger G. Functional analysis of a duplication (p.E63_D69dup) in the switch II region of HRAS: new aspects of the molecular pathogenesis underlying Costello syndrome. Hum Mol Genet. 2013; 22:1643–1653. [PubMed: 23335589]

Nosan G, Bertok S, Vesel S, Yntema HG, Paro-Pamjan D. A lethal course of hypertrophic cardiomyopathy in Noonan syndrome due to a novel germline mutation in the *KRAS* gene: case study. Croat Med J. 2013; 54:574–578. [PubMed: 24382853]

Niihori T, Aoki Y, Narumi Y, Neri G, Cavé H, Verloes A, Okamoto N, Hennekam RC, Gillessen-Kaesbach G, Wieczorek D, Kavamura MI, Kurosawa K, Ohashi H, Wilson L, Heron D, Bonneau D, Corona G, Kaname T, Naritomi K, Baumann C, Matsumoto N, Kato K, Kure S, Matsubara Y. Germline KRAS and BRAF mutations in cardio-facio-cutaneous syndrome. Nat Genet. 2006; 38:294–296. [PubMed: 16474404]

Polakis P, McCormick F. Structural requirements for the interaction of p21ras with GAP, exchange factors, and its biological effector target. J Biolog Chem. 1993; 268:9157–9160.

Rosenberger G, Meien S, Kutsche K. Oncogenic HRAS mutations cause prolonged PI3K signaling in response to epidermal growth factor in fibroblasts of patients with Costello syndrome. Hum Mutat. 2009; 30:352–362. [PubMed: 19035362]

Runtuwene V, van Eekelen M, Overvoorde J, Rehmann H, Yntema HG, Nillesen WM, van Haeringen A, van der Burgt I, Burgering B, den Hertog J. Noonan syndrome gain-of-function mutations in NRAS cause zebrafish gastrulation defects. Dis Model Mech. 2011; 4:393–399. [PubMed: 21263000]

Scheffzek K, Ahmadian MR. GTPase activating proteins: structural and functional insights 18 years after discovery. Cell Mol Life Sci. 2005; 62:3014–3038. [PubMed: 16314935]

Scheffzek K, Ahmadian M, Kabsch W, Wiesmuller L, Lautwein A, Schmitz F, Wittinghofer A. The Ras-RasGAP complex: structural basis for GTPase activation and its loss in oncogenic Ras mutants. Science. 1997; 277:333–338. [PubMed: 9219684]

Scheffzek K, Ahmadian MR, Wiesmuller L, Kabsch W, Stege P, Schmitz F, Wittinghofer A. Structural analysis of the GAP-related domain from neurofibromin and its implications. Embo J. 1998; 17:4313–4327. [PubMed: 9687500]

Schuhmacher AJ, Guerra C, Sauzeau V, Canamero M, Bustelo XR, Barbacid M. A mouse model for Costello syndrome reveals an Ang II-mediated hypertensive condition. J Clin Invest. 2008; 118:2169–2179. [PubMed: 18483625]

Seeburg PH, Colby WW, Capon DJ, Goeddel DV, Levinson A. Biological properties of human c-Ha-ras1 genes mutated at codon 12. Nature. 1984; 312:71–75. [PubMed: 6092966]

Sanger Institute. [Accessed January 6th, 2015] Catalogue of Somatic Mutations in Cancer. 2007. Distribution of somatic mutations in HRAS. www.sanger.ac.uk

Stieglitz B, Bee C, Schwarz D, Yildiz O, Moshnikova A, Khokhlatchev A, Herrmann C. Novel type of Ras effector interaction established between tumour suppressor NORE1A and Ras switch II. Embo J. 2008; 27:1995–2005. [PubMed: 18596699]

Sung YJ, Carter M, Zhong JM, Hwang YW. Mutagenesis of the H-ras p21 at glycine-60 residue disrupts GTP-induced conformational change. Biochemistry. 1995; 34:3470–3477. [PubMed: 7880841]

Sung YJ, Hwang MC, Hwang YW. The dominant negative effects of H-Ras harboring a Gly to Ala mutation at position 60. J Biol Chem. 1996; 271:30537–30543. [PubMed: 8940023]

Sol-Church K, Stabley DL, Nicholson L, Gonzalez IL, Gripp KW. Paternal Bias in Parental Origin of *HRAS* Mutations in Costello Syndrome. Hum Mutat. 2006; 27:736–741. [PubMed: 16835863]

Sol-Church K, Stabley DL, Demmer LA, Agbulos A, Lin AE, Smoot L, Nicholson L, Gripp KW. Male-to-male transmission of Costello syndrome: G12S HRAS germline mutation inherited from a father with somatic mosaicism. Am J Med Genet Part A. 2009; 149A:315–321. [PubMed: 19206176]

Stacey DW, Feig LA, Gibbs JB. Dominant inhibitory Ras mutants selectively inhibit the activity of either cellular or oncogenic Ras. Molecular and cellular biology. 1991; 11:4053–4064. [PubMed: 2072908]

Tyner JW, Erickson H, Deininger MW, Willis SG, Eide CA, Levine RL, Heinrich MC, Gattermann N, Gilliland DG, Druker BJ, Loriaux MM. High-throughput sequencing screen reveals novel, transforming RAS mutations in myeloid leukemia patients. Blood. 2009; 113:1749–1755. [PubMed: 19075190]

Vetter IR, Wittinghofer A. The guanine nucleotide-binding switch in three dimensions. Science. 2001; 294:1299–304. [PubMed: 11701921]

Zampino G, Pantaleoni F, Carta C, Cobellis G, Vasta I, Neri C, Pogna EA, De Feo E, Delogu A, Sarkozy A, Atzeri F, Selicorni A, Rauen KA, Cytrynbaum CS, Weksberg R, Dallapiccola B, Ballabio A, Gelb BD, Neri G, Tartaglia M. Diversity, parental germline origin, and phenotypic spectrum of de novo HRAS missense changes in Costello syndrome. Hum Mutat. 2007; 28:265–272. [PubMed: 17054105]

Zenker M, Lehman K, Schulz AL, Barth H, Hansmann D, Koening R, Korinthenberg R, Kreiss-Nachtsheim M, Meinecke P, Morlot S, Mundlos S, Quante AS, Raskin S, Schnabe D, Wehner LE, Kratz CP, Hern D, Kutsche K. Expansion of the genotypic and phenotypic spectrum in patients with KRAS germline mutations. J Med Genet. 2007; 44:131–135. [PubMed: 17056636]

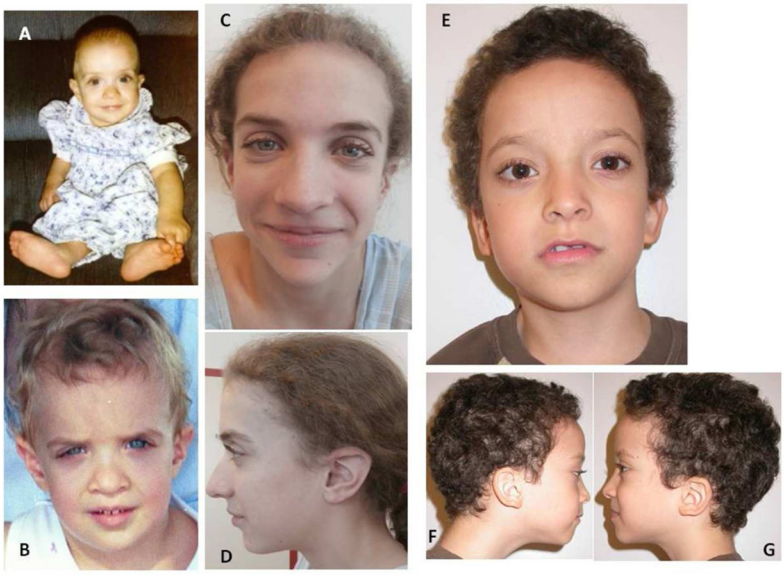

Figure 1.

Patient 1 at age 11 months (A), 3 years (B) and 15 years (C and D), note tall forehead, telecanthus and mild ptosis, wide mouth and curly hair; Patient 2 (E–G) at age 8 years, note tall forehead, apparent hypertelorism and curly hair.

Figure 2.

Facial photographs of Patient 3 (A, B) at age 13 months; facial photographs of Patient 4 (C, D), lesion on inner surface of lower lip (E) and feet with callouses and deep plantar creases (F, G).

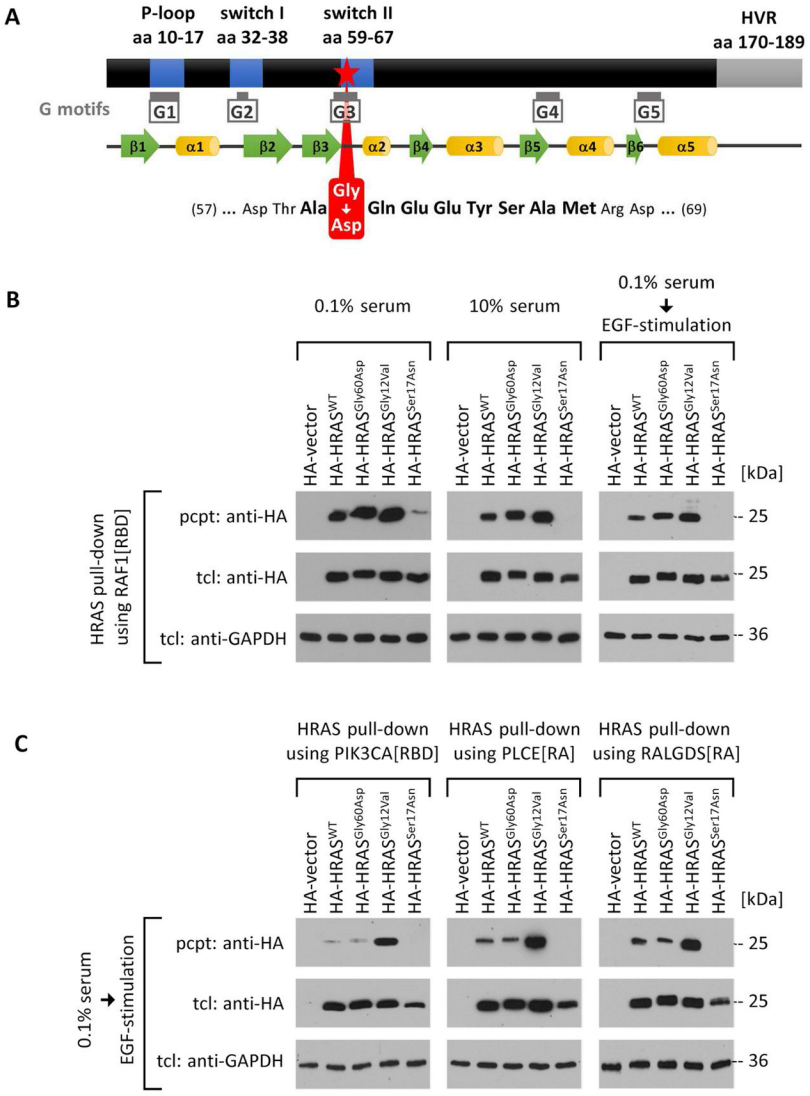

Figure 3.

$HRAS^{Gly60Asp}$ strongly co-precipitates with RAF1, but not with PIK3CA, PLCE1 or RALGDS. **A.** Schematic representation of HRAS and position of the p.Gly60Asp amino acid change. Motifs representing the P-loop, switch I and II regions as well as the hypervariable region (HVR) are highlighted and amino acids (aa) constituting these motifs are given. Below RAS-specific five conserved G motifs (G1–G5, gray boxes) are depicted. Secondary structural elements of HRAS are shown as green arrows and yellow cylinders representing β-sheets and α-helices, respectively. Position of residue glycine 60 in HRAS switch II amino acids sequence (bold letters) is given. **B.** COS-7 cells transiently expressing $HA\text{-}HRAS^{WT}$ (wildtype), $HA\text{-}HRAS^{Gly60Asp}$, $HA\text{-}HRAS^{Gly12Val}$ or $HA\text{-}HRAS^{Ser17Asn}$ were cultured under serum-starved condition (0.1% serum), normal growth condition (10% serum), or serum-starved condition followed by 20 min stimulation with 10 ng/ml EGF (0.1% serum→EGF-stimulation). For control purpose cells were transfected with empty vector. GTP-bound HA-tagged HRAS protein variants were precipitated from cell extracts

using GST-RAF1 [RBD]. Precipitated HA-HRAS (pcpt) and amount of HA-HRAS protein in total cell lysates (tcl) was detected by immunoblotting using anti-HA antibody. Cellular extracts were probed with anti-GAPDH antibody to control for equal loading. Data shown are representative of three independent experiments. **C**. Same procedure as described in B, except cells were cultured under serum-starved condition followed by 20 min stimulation with 10 ng/ml EGF (0.1% serum→EGF-stimulation) and GTP-bound HRAS protein variants were precipitated by using GST-PIK3CA[RBD], GST-PLCE1[RA], or GST-RALGDS[RA] fusion proteins. Data shown are representative of three independent experiments.

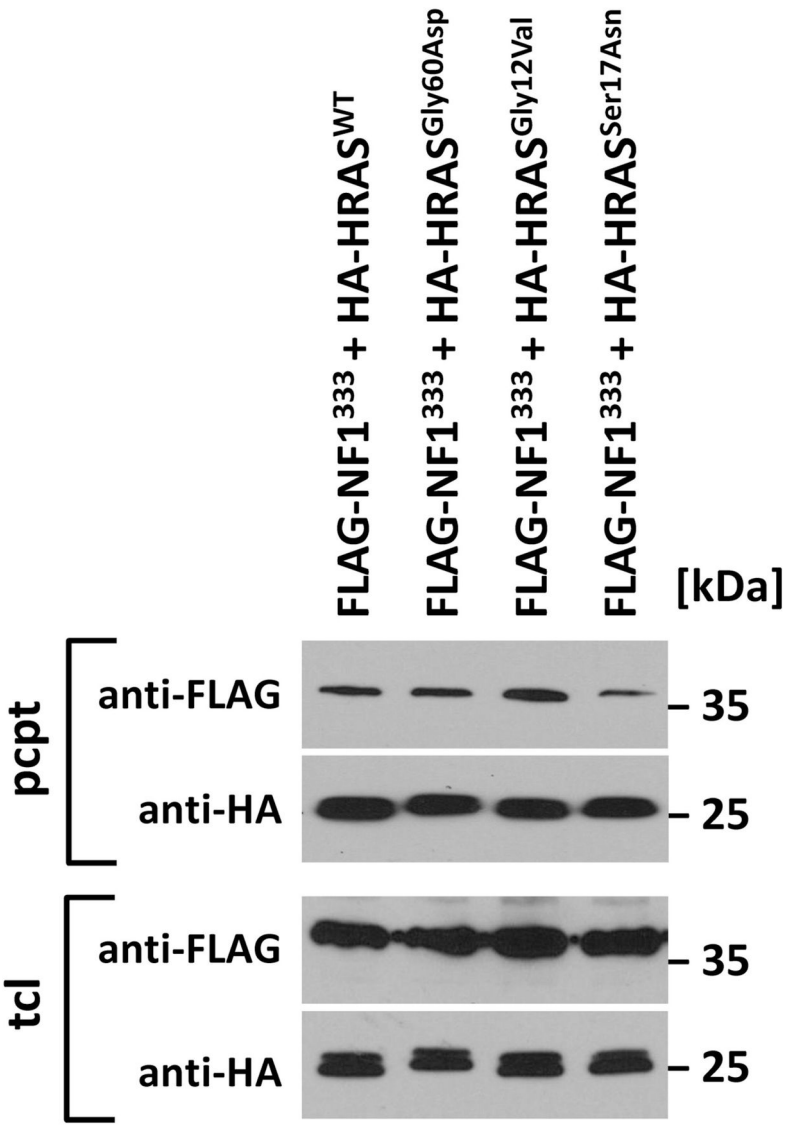

Figure 4.

The p.Gly60Asp mutation does not affect binding of HRAS with NF1 GAP. COS-7 cells were transfected with expression constructs as indicated and cultured under basal growth conditions (10% serum). Vector control is shown in lane 1. HA-tagged HRAS protein variants were immunoprecipitated from cell extracts using anti-HA-conjugated agarose beads. Upon SDS PAGE and western blotting, precipitates (pcpt) and total cell lysates (tcl) were probed with anti-HA and anti-FLAG antibodies. Data shown are representative of three independent experiments.

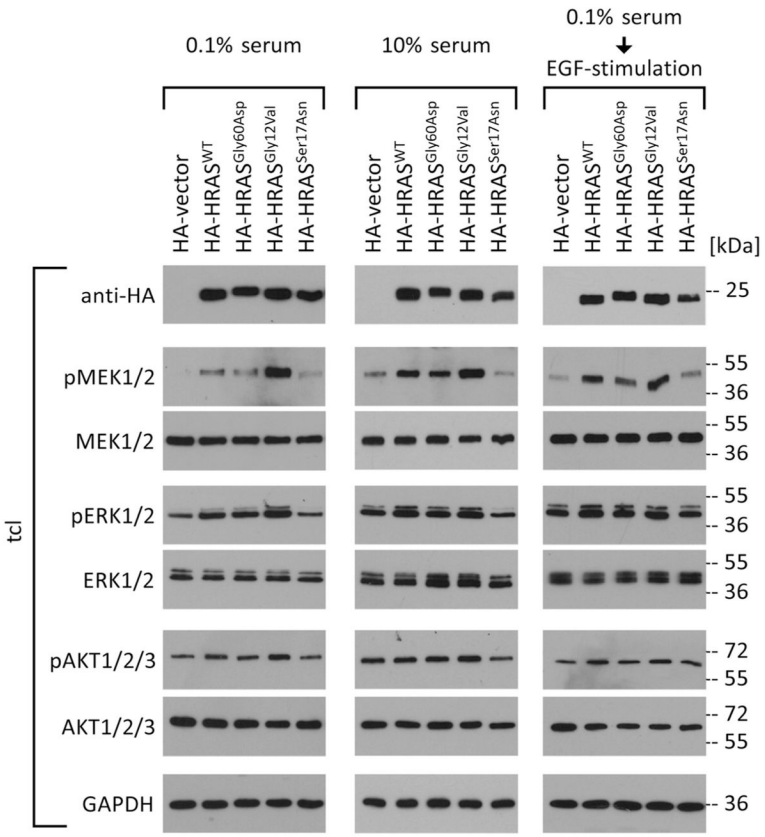

Figure 5.

Expression of HRAS^{Gly60Asp} does not enhance phosphorylation of MEK1/2, ERK1/2 and AKT. COS-7 cells were transfected with constructs expressing HA-HRAS^{WT}, HA-HRAS^{Gly60Asp}, HA-HRAS^{Gly12Val}, or HA-HRAS^{Ser17Asn} as indicated. For control purpose cells were transfected with empty vector. Cells were cultured under serum-starved condition (0.1% serum), normal growth condition (10% serum), or serum-starved condition followed by 20 min stimulation with 10 ng/ml EGF (0.1% serum→EGF-stimulation). Total cell lysates (tcl) were analyzed by immunoblotting using specific antibodies. The representative autoradiographs show levels of phospho-MEK1/2, total MEK1/2, phospho-ERK1/2, total ERK1/2, phospho-AKT1/2/3 and total AKT1/2/3. Expression of HRAS protein variants was verified by probing cellular extracts with anti-HA antibody and anti-GAPDH antibody was used to control for equal loading. One representative data set out of three independent experimental series is shown.

Am J Med Genet A. Author manuscript; available in PMC 2016 April 13.

Table I

Phenotypic Findings in Individuals with HRAS p.Gly60Asp, Compared to Those with the Common HRAS p.Gly12Ser, p.Gly13Cys and the Rare HRAS p.Thr58Ile Associated with an Attenuated Phenotype

	Individual 1	Individual 2	Individual 3	Individual 4	Attenuated Costello syndrome HRAS p.The58Ile	Costello syndrome HRAS p.Gly13Cys	Typical Costello syndrome HRAS p.Gly12Ser
Failure to thrive	−	−	−	−	+/−	+	+
Macrocephaly	75th–90th centile	+	90th centile		+	+	+
Height less than −2SD below mean for age	3rd centile	5th centile	50th centile	50–75th centile	−	+/−	+
Hypertrophic cardiomyopathy	−	−	Mildly thickened left ventricle	None known *	+/−	+	+
Other cardiac findings	Atrial tachycardia	Tachycardia	dysplastic pulmonic valve, mild stenosis	None known *	Double-chambered right ventricle; Mitral valve prolapse	ASD; no multifocal atrial tachycardia	Pulmonic stenosis; ASD; multifocal atrial tachycardia
Limited range of motion in elbows	−	−	−	−	+/−	−	+
Ligamentous laxity	−	Small joints, thumb	−		+/−	+/−	Small joints, thumb
Deep palmar/plantar creases	−	−	−	+	+/−	+/−	+
Developmental delay	−	+	−	−	+/−	+/−	ID
Hypotonia	−	+	−	−	+/−	+	+
Neurologic and behavior issues	−	ADHD; Behavior issues	−	Learning differences	ADHD, tremor Behavior problems	Anxiety	Sleep disturbance; anxiety
Eye findings	Nystagmus	?	Ptosis	−	Strabismus; nystagmus	Strabismus; nystagmus	Strabismus; nystagmus
Papillomata	−	−	−	oral lesion	−	−	+
Malignant tumor	−	−	−	−	−	−	+/−
Other	Pectus excavatum; delayed puberty	−			Pyloric stenosis	Loose anagen hair; dolichocilia	Coarse facial features; curly hair

* Echocardiogram and EKG not performed

+, present; −, absent; ASD, atrial septal defect; ADHD, attention deficit hyperactivity disorder; ID, intellectual disabiliy